

Adversarial Training with Natural Transformation

Shuo Wang, Surya Nepal, Marthie Grobler, Kristen Moore
CSIRO
Melbourne, Australia
shuo.wang@csiro.au

Lingjuan Lyu
National University of Singapore
Singapore
lyulj@comp.nus.edu.sg

Abstract

Previous robustness approaches for deep learning models such as data augmentation techniques via data transformation or adversarial training cannot capture real-world variations that preserve the semantics of the input, such as a change in lighting conditions. To bridge this gap, we present NaTra, an adversarial training scheme that is designed to improve the robustness of image classification algorithms. We target attributes of the input images that are independent of the class identification, and manipulate those attributes to mimic real-world natural transformations (NaTra) of the inputs, which are then used to augment the training dataset of the image classifier. Specifically, we apply Batch Inverse Encoding and Shifting to map a batch of given images to corresponding disentangled latent codes of well-trained generative models. Latent Codes Expansion is used to boost image reconstruction quality through the incorporation of extended feature maps. Unsupervised Attribute Directing and Manipulation enables identification of the latent directions that correspond to specific attribute changes, and then produce interpretable manipulations of those attributes, thereby generating natural transformations to the input data.

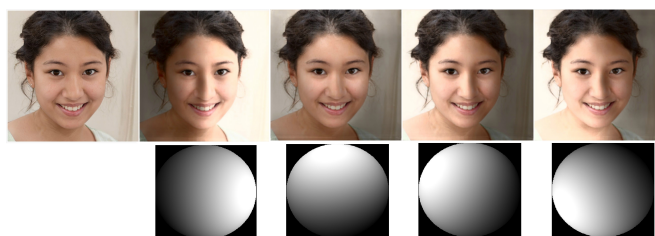
We demonstrate the efficacy of our scheme by utilizing the disentangled latent representations derived from well-trained GANs to mimic transformations of an image that are similar to real-world natural variations (such as lighting conditions or hairstyle), and train models to be invariant to these natural transformations. Extensive experiments show that our method improves generalization of classification models and increases its robustness to various real-world distortions.

1. Introduction

The success of adversarial attacks has demonstrated the susceptibility of deep learning models to making incorrect predictions with high confidence, due to small but carefully chosen deviations to the input, i.e. adversarial perturbations

[6, 12, 23, 35]. Figure 1 shows that even small variations in the angle of light irradiation and face rotation, background, and exposure conditions for images can result in drastic degradation in the performance of well-trained deep neural networks.

These examples reveal that state-of-the-art deep learning models sometimes fail to generalize to small variations of the input. A possible reason for this is that the representations learnt by them are not good and the robustness of the learned deep neural networks is limited. If deviations exist between training and testing instances, it is commonplace for models to fail in catastrophic ways.



(a) The original image is at the top left; the rest of the images are misclassified variations under various angles of light irradiation.



(b) The original image is at the top left; the rest of the images are misclassified variations, such as hairstyle, face orientation, exposure condition, background, visual orientation, eyebrows, etc.

Figure 1. VGGFace model can be deceived by image transformations that mimic real world distortions.

On the one hand, approaches to improve robustness have been found to fall short of their goals, in particular data augmentation techniques via data transformation. Transformations such as cropping, flipping, scaling, color jittering,

and region masking (Cutout) are commonly used augmentations for vision models. Training on the corrupted data only forces the memorization of such corruptions, and as a result these models fail to generalize to new corruptions [36, 11]. Works such as Mixup [41] or AutoAugment [9] pave the way to further improvements, but still require intricate fine-tuning to succeed in practice. Furthermore, these transformations tend to destroy the image semantics.

On the other hand, prior works [12, 29, 20, 39] have shown that adversarial training [26] is effective in building models that are robust to adversarial perturbations. Given a perturbation threshold, ϵ , adversarial training intends to minimize the loss of robustness, the worst-case loss within the ϵ -ball around each example, leading to a min-max optimization problem. However, such perturbation fails to capture real-world variations that preserve the semantics of the input, such as a change in lighting conditions.

This paper focuses on training models to be more robust to natural transformations that mimic real world distortions while preserving the semantic attributes of input images, such as variations to the subject’s face orientation, degree of eye opening, or the perspective orientation of objects in Figure 1. Instead of the conventional data augmentation and adversarial training on L_p -norm bounded perturbations, we achieve this robustness via controllable attributes editing on given high-fidelity inputs.

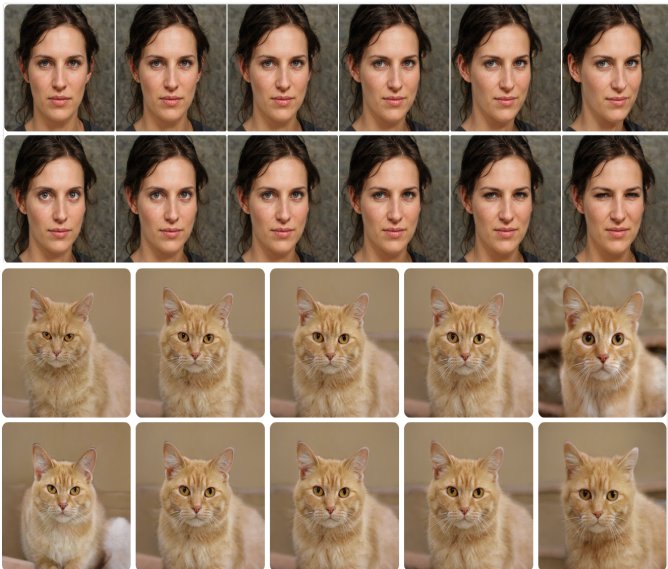


Figure 2. The demonstration of natural transformations that mimic four real-world variations, i.e. face orientation and eye-opening degree for human, angle of elevation and body orientation for cat.

In terms of generating high-fidelity images, Generative Adversarial Networks (GANs) have paved a feasible path towards generating high-fidelity images and producing a disentangled latent representation with a rich linear struc-

ture, e.g. StyleGAN [21, 22] and BigGAN [5]. However, since the standard GAN model was initially designed for synthesizing images from random noises, applying trained GAN models to real image post-processing remains challenging. Existing methods commonly invert a given image back to the latent space either by back-propagating one by one, or by learning an additional encoder. However, the efficiency and reconstruction quality from both of these methods are far from ideal. The main challenges in the manipulation of selected attributes of given images while preserving the other details include: (1) *obtaining an efficient reverse function to map massive images to the disentangled latent space of a well-trained generator model, especially for high resolution image generators*; (2) *recovering as many details as possible of any arbitrary real image in the reversed latent codes using all the possible composition knowledge learned in the deep generative representation*; (3) *finding a proper latent direction that corresponds to the latent codes, that changes only the desired attribute, and to do so with minimum supervision, or ideally in an unsupervised manner*. This work address these challenges, and we summarise our contributions as follows:

1. We use *Batch Inverse Encoding and Shifting* (BIES) to map massive given images to the corresponding disentangled latent codes of well-trained generative models at one time, which enables the inverse function of the generator to be accurately learned via an encoder in an end-to-end and unsupervised manner.
2. We adopt *Latent Codes Expansion* (LCE) to boost image reconstruction quality, and apply *Unsupervised Attribute Directing and Manipulating* (ADM) to find latent directions towards specific attribute change and then obtain interpretable manipulation for generating nature transformations.
3. We develop a new framework to leverage the disentangled latent codes of a well-trained generative model to generate a set of *natural transformation* ((NaTra)) copies for each given image. This enables us to improve robustness via adversarial training on the natural data augmentation in a purely data-driven fashion.
4. We conduct extensive experiments on CelebA-HQ, LSUN datasets, and compare NaTra augmentation with the conventional data augmentation to demonstrate under which conditions NaTra achieves higher accuracy. We empirically demonstrate that accuracy is not necessarily at odds with robustness, once we consider natural variations other than L_p -norm bounded variations.

2. Related work

2.1. StyleGAN

StyleGAN is a generator architecture for generative adversarial networks proposed by Karras et al. [21] and improved in [22]. Formally, the StyleGAN architecture is composed of two stages. The first stage takes a latent variable $z \sim N(0, 1)$ that is not necessarily disentangled and projects it into a disentangled latent space $w = \text{map}(z)$. The second stage synthesizes an image x from the disentangled latents w using a decoder $x = \text{dec}(w)$. The intermediate latent variable z provides some level of disentanglement that affects image generation at different spatial resolutions which allows us to control the synthesis of an image.

To reverse the generation process, existing approaches fall into two types. One is to directly optimize the latent code by minimizing the reconstruction error through back-propagation [8, 24, 1]. The other is to train an extra encoder to learn the mapping from the image space to the latent space [4, 43, 30, 25]. However, the reconstructions achieved by both methods are far from ideal, especially with high resolution images.

2.2. L_p -norm perturbations and Adversarial robustness beyond L_p -norm

Generating pixel-level adversarial perturbations has been and remains extensively studied [27, 12, 35, 26, 29]. Most works focus the robustness of classifiers under L_p -norm bounded perturbations. In particular, it is expected that a robust classifier should be invariant to small perturbations in the pixel space (as defined by the L_p -norm). However, robustness to semantically meaningful perturbations remains a largely unexplored problem.

[10] and [19] explored geometric transformations such as rotations and translation of images. Early works (e.g., Baluja and Fischer [2]) also demonstrated that it is possible to go beyond analytically defined variations by using generative models to create perturbations. [33, 38] used a pre-trained AC-GAN [28] to generate perturbations; and they demonstrated that it is possible to generate semantically relevant perturbations for tasks such as MNIST, SVHN and CELEBA. Lastly, [31] have attempted to generate adversarial examples by interpolating through the attribute space defined by a generative model. With the exception of [18], in which the authors strongly limit semantic variations by keeping the perturbed image close to its original counterpart, there has been little to no work demonstrating robustness to large semantically plausible variations. As such, the effect of training models to be robust to such variations is unclear. To the best of our knowledge, this paper is the first to analyze the difference between adversarial training and data augmentation in the space of semantically meaningful variations.

3. Robustness via Adversarial Training on Natural Transformation

3.1. Problem Definition

Adversarial training has become one of the most effective methods for improving robustness of neural networks. Adversarial training in this study can be considered as a data augmentation technique that fine-tunes DNNs on additional natural transformations of natural inputs to improve the robustness of the classifier to feature variations. Essentially, we implement an autoencoder scheme to conduct such real-world natural transformations. *Batch Inverse Encoding and Shifting – BIES* is used to map massive given images to corresponding disentangled latent codes of well-trained generative models at one time, i.e. $\text{enc} : X \rightarrow Z$. The well-trained generator can be used as a decoder to reconstruct these manipulated latent codes to corresponding transformed images, i.e., $\text{dec} : Z \rightarrow X$. Disentanglement means that factorized attributes could be recognized and manipulated from encoded latent codes. *Latent Codes Expansion – LCE* is applied to boost the image reconstruction quality. *Unsupervised Attribute Directing and Manipulating – ADM* is implemented to find latent directions towards specific attributes change via conducting principle analysis on the latent codes, and then obtain interpretable manipulation via adding bounded perturbation into the corresponding latent codes along the corresponding direction for generating nature transformations. Therefore, we can conduct various T_s by reconstruction of the manipulated corresponding latent codes.

Formally, for a C-class ($C \geq 2$) classification problem, given a dataset $\{x_i, y_i\}_{i=1, \dots, n}$ with (x_i, y_i) is a pair of example and corresponding label from the data distribution $D \subset X \times Y$, n is the number of training examples, a DNN classifier f_θ parametrized by θ , we aim to improve its robustness against variations derived from some natural transformations $T_{s_{1:M}} : \text{dec}(z = \text{enc}(x)) \mapsto \text{dec}(\tilde{z})$ in terms of a set of desired semantic features $s \in S$ via manipulating the corresponding latent codes after encoding x_i . Namely, we aim to refine the model parameters θ by solving the following min-max optimization problem:

$$\min_{\theta} \frac{1}{n} \sum_{i=1}^n \max_{\substack{T_s \\ z_i^s \in B(\epsilon, z_i^s)}} L(f_\theta(T_s(x)), y), \forall s \in S \quad (1)$$

where L can be any loss function (e.g. cross entropy loss or 0-1 loss in the context of classification tasks $\mathbf{1}(f_\theta(T_s(x)) \neq y)$). A specific transformation $T_s \in T_{s_{1:M}}$ is expected to produce real-world natural transformation on a semantic feature s from a set of desired semantic features S , $\tilde{z}_i \in B(\epsilon, z_i) := \{z_i : \|z_i - \tilde{z}_i\|_p \leq \epsilon\}$ denotes the L_p -norm ball centered at original latent codes z_i with radius ϵ . For the robust classifier $f_\theta : X \rightarrow Y$, we would like

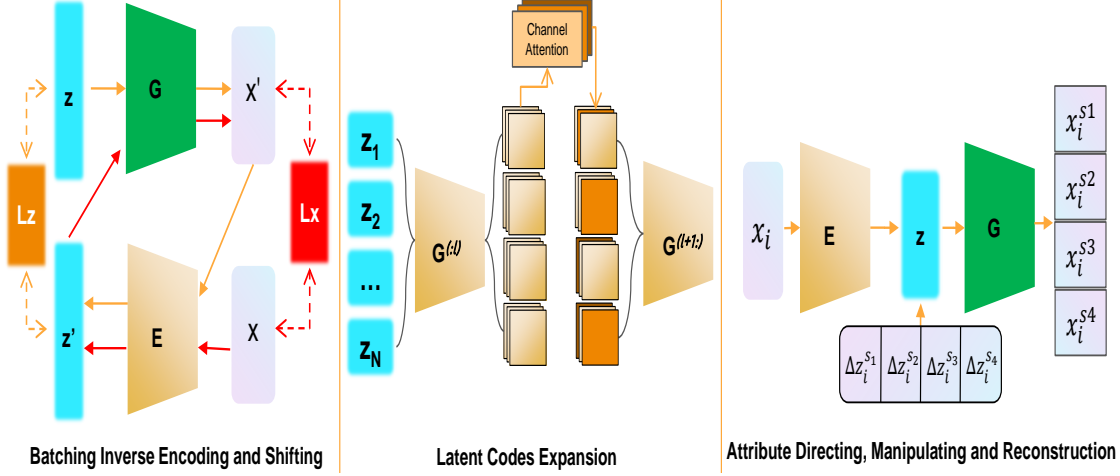


Figure 3. The scheme of natural transformation (NaTra).

that $f_\theta(T_s(x)) = f_\theta(x), \forall s \in S$. In particular, comprehensive task-irrelevant feature variations should be well investigated. For example, a face recognition classifier should not be affected by changes in the lighting conditions, background, or facial expression.

Based on the disentanglement, given a classification task, e.g., face recognition, that predicts the label y , $\tilde{z}_\mathcal{O}^s$ denotes the manipulated latent codes along the direction of a specific task-irrelevant semantic feature s , such as the facial expression. Given an example and labelled pair (x, y) , we can obtain the disentangled latent codes via $z = enc(x)$, then for any task-irrelevant feature s , the prediction label will not be affected when modifying corresponding z^s part of z . The transformation T_s on a specific semantic feature s can be reflected in the perturbed latent code $\tilde{z}_\mathcal{O}^s$. Formally, given the desired semantic feature set S , the *natural transformation* for a specific instance x with label y is produced via

$$T = \{(T_s | T_s(x) = dec(\tilde{z}_\mathcal{O}^s), s.t. f(dec(z)) = f(dec(\tilde{z}_\mathcal{O}^s))\}, \quad (2)$$

$$\forall s \in S \text{ and } \tilde{z}_\mathcal{O}^s \in B_{(\epsilon, z)}.$$

Therefore, the robust classifier f^* should predict a given x with the correct label while resisting bounded variations on its latent codes and for all desired task-irrelevant features.

A robust model f_θ^* to T means there is no bounded perturbation on any T_s would cause the misclassification of f_θ^* . Formally, the robustness depends on parameters θ^* that satisfies Equation 3.

$$\theta^* = \underset{\theta}{argmax} E_{(x,y) \in D} [\underset{s \in S, \tilde{z}_\mathcal{O}^s \in B_{(\epsilon, z)}}{max} L(f_\theta(dec(\tilde{z}_\mathcal{O}^s)), y)] \quad (3)$$

Solving Equation 3 requires solving the corresponding inner-maximization problem for each $\tilde{z}_\mathcal{O}^s$ within bounded

ball:

$$\tilde{z}_\mathcal{O}^* = \underset{s \in S, \tilde{z}_\mathcal{O}^s \in B_{(\epsilon, z)}}{argmax} L(f_\theta(dec(\tilde{z}_\mathcal{O}^s)), y) \quad (4)$$

L can be replaced with the cross-entropy loss \hat{L} :

$$\hat{L}(f_\theta(x), y) = -\log([f_\theta(x)]_y) \quad (5)$$

where $[a]_i$ returns the i^{th} coordinate of a . Gradient ascent steps are then interleaved with projection steps for a given number of iterations K . $\tilde{z}_\mathcal{O}^*$ can be estimated by recursion interleaved with projection steps for K iterations for each s , i.e. $\tilde{z}_\mathcal{O}^{(K)}$:

$$\tilde{z}_\mathcal{O}^{(k+1)} = proj_{Z_\mathcal{O}}(\tilde{z}_\mathcal{O}^{(k)} + \alpha \nabla_{\tilde{z}_\mathcal{O}^{(k)}} \hat{L}(f_\theta(dec(\tilde{z}_\mathcal{O}^{(k)})), y)) \quad (6)$$

where α is a constant step-size and $proj_A(a)$ is a projection operator that project a onto A as [13].

The baseline approach to achieve the robustness is to fine-tune the model f on the additional data that consists of a set of natural transformations $NT_x^s, \forall s \in S$ with bounded perturbation for each training instance with correct label. After finding the latent direction for a specific task-irrelevant semantic feature, we can construct the natural transformation set in terms of the features via editing the latent codes via the decided direction. Consequently, the natural transformation augmentation is defined as:

$$NT_x = \{(T_s(x), y) | T_s(x) = dec(\tilde{z}_\mathcal{O}^s), s.t. f(dec(z)) \neq f(dec(\tilde{z}_\mathcal{O}^s))\}, \quad (7)$$

$$\forall s \in S \text{ and } \tilde{z}_\mathcal{O}^s \in B_{(\epsilon, z)}.$$

3.2. Batch Inverse Encoding and Shifting

By learning to map into the latent space of a pre-trained image generator, we leverage both its state-of-the-art generative power, and its disentangled and expressive latent

space, without the burden of training it. We train an additional encoder to obtain the inverse mapping from massive given images to the latent space of a well-trained generator network. Such an encoder provides a fast solution of image embedding by performing a forward pass through the encoder neural network.

Given a generator network $g_\nu(z)$ (i.e. $dec_\nu(z)$) that maps the latent space Z to the data space X , BIES aims to learn an encoder network $enc_\eta(x)$ that maps the image x from the data space to the latent space Z of $g_\nu(z)$. The architecture of BIES is shown at the left of Figure 3. The first goal of BIES is the ability to reverse the latent representation of randomly generated samples. For a given random z , the generator generates an image x' that is then fed into the encoder network to obtain an estimated latent codes z' . We minimize the objective in Equation 8 to minimize the error between the estimated $z' = enc_\eta(g_\nu(z))$, and the initial z .

$$\eta^* = \underset{\eta}{\operatorname{argmin}}(E_{z \sim P(Z)} \|z - enc_\eta(g_\nu(z))\|_2^2) \quad (8)$$

The second goal of BIES from the model is to reconstruct real images from z' with good quality. For a given image x and its encoded z' , the generator g is used to reconstruct its corresponding image $x' = g_\nu(enc_\eta(x))$. We use the objective in Equation 10 to minimize the error between x' and x . To improve the reconstruction quality, both pixel-wise MAE error (low-level) and perceptual error (high-level) are used to better steer the optimization. The perceptual loss is evaluated on the the l_1 distance between the perceptual features $V_l(\cdot)$ extracted at the i^{th} layer of a trained VGG-16 network.

$$\eta^* = \underset{\eta}{\operatorname{argmin}}(E_{x \sim P_{data}}(\gamma_1 \|x - g_\nu(enc_\eta(x))\|_2^2 + \gamma_2 \sum_l \|V_l(x) - V_l(g_\nu(enc_\eta(x)))\|_1)) \quad (9)$$

The encoder’s parameters are updated twice in each iteration in terms of Equation 10 and 8, respectively. The input of the encoder is alternatively either real or generated images, and the input of the generator is alternatively either a randomly generated or an encoded latent vector as the input. During training, only the parameters η are updated, while the well-trained generator is fixed. The encoder is trained using a pre-trained generator without facing stability problems.

After the encoder is well trained, the generator will be fine-tuned using the instances in the target domains, to shift the weights of the generator as a decoder towards the target distribution. We fix the encoder while updating the weights of the generator to match the targeted generated image. The pre-trained generator will be shifted toward the targeted domain after slightly updating its weights on the targeted domain images. For each image, we fix its encoded latent

codes and update the weights of g , dragging the nearest neighbor of the pre-trained generator manifold closer to the target manifold. The objective function can be defined as:

$$g^* = \underset{\nu}{\operatorname{argmin}}(E_{x \sim P_{data}}(\gamma_1 \|x - g_\nu(enc_\eta(x))\|_2^2 + \gamma_2 \sum_l \|V_l(x) - V_l(g_\nu(enc_\eta(x)))\|_1)) \quad (10)$$

Equation 10 is used as the loss function for fine-tuning g .

3.3. Latent Codes Expansion

Given a target image x , the BIES can be applied to reverse the generation process by encoding the latent code to recover x . However, it is hard to reconstruct an ideal image by optimizing a single latent code vector, which may not be enough to recover all the details of a particular image. In this strategy, we embed given images into an extended latent space, which is a concatenation of multiple latent vectors, used for revealing multiple feature maps and improving image reconstruction quality [15]. These extended latent vectors will be composed of some intermediate layer of the generator, in terms of adaptive channel importance to better recover the input image. Namely, latent codes z are extended to z^+ , and they are incorporated together via merging corresponding intermediate feature maps with the attention mechanism. N latent codes $\{z^i\}_{i=1}^N$ are implemented to reverse given inputs, each of which can help reconstruct some sub-regions of the target image. In particular, a specific layer (with index l) of generator $g(\cdot)$ is selected to divide g into two sub-networks, i.e., $g_h^l(\cdot)$ and $g_r^l(\cdot)$. For any z^i , we can extract the corresponding spatial feature $g^l(\cdot) = \sum_i^N g_h^l(z_i)$ for further composition. Each z^i is expected to recover some particular regions of the target image. It has been demonstrated that different channels of the generator control different visual concepts such as objects and textures [3]. Consequently, the attention mechanism is used to allocate channel importance α_i for each z^i to encourage them align with different semantics. Here, $\alpha_i \in R^C$ is a C -dimensional vector to reveal the importance of the corresponding channel of the feature map, and C is the number of channels in the l -th layer of $g(\cdot)$. The reconstructed image can be generated with $x' = g_r(\sum_{i=1}^N g^l \odot \alpha_i)$ where \odot denotes the channel-wise multiplication as $\{g^l \odot \alpha_i\}_{h,w,c} = \{g^l\}_{h,w,c} \times \{\alpha_i\}_c$. Here, h and w indicate the spatial location, while c stands for the channel index.

StyleGANs have two kind of latent space, i.e. initial latent space Z and the intermediate latent space W . The 512-dimensional vectors $w \in W$ are mapped from the 512-dimensional vectors $z \in Z$ by a fully connected neural network M . The extended latent space W^+ is a concatenation of 18 different 512-dimensional w vectors, one for

each layer of the StyleGAN architecture that can receive input via adaptive instance normalization (AdaIN) [17].

3.4. Unsupervised Attribute Directing, Manipulating and Reconstruction (ADMR)

To identify latent directions corresponding to important semantic features, a dimensionality reduction approach based on uniform manifold approximation and projection (UMAP) is implemented in the activation space. Layer-wise manipulation of the GANs are then performed to produce edits in the input image that are interpretable in terms of chosen semantic features [16]. ADMR has two advantages: it is simple and unsupervised.

3.4.1 Attribute Directing

The first step is to discover valuable directions in the latent space for some semantic features. Generally, the GAN network consists of a sequence of layers g^1, \dots, g^L . The first layer adopts the latent vector as input and provides a set of activations $o_1 = g^{(1)}(z)$. The remaining layers each produce activations as a function of the previous layer’s output. The last layer’s output $x' = g^{(L)}(o_{L-1})$ is an image. For StyleGAN [21, 22], the first layer takes a constant input, o_0 . The output is controlled by a non-linear function of z as input to intermediate layers, $o_i = g^{(i)}(o_{i-1}, w = M(z))$ where M is an 8-layer multilayer perceptron. For the BigGAN [5], the intermediate layers also use the latent vector as input, $o_i = g^{(i)}(o_{i-1}, z)$.

The principal components of activation tensors on the first few layers of the generator represent important factors of variation ([16]). ADMR aims to recognize the principal axes of $p(w)$ or $p(z)$. Generally, K random latent codes tensors are sampled, i.e. $z_{\{1:K\}}^{D*N}$ where D is the dimension of each latent codes (e.g. 512), N is the extension scale for Latent Codes Expansion, and K is the number of sampling. The dimensionality reduction algorithm UMAP is used to calculate the principal components of these latent codes, resulting in a low-rank basis V .

For StyleGAN, we then figure out the corresponding $w^i = M(z^i)$ values. We can edit the image, with the encoded latent codes w , via $w' = w + Vr, x' = g(o_0, w')$ where each entry r_i of r is a separate control parameter.

For BigGAN, we first perform UMAP at on the intermediate network layer i of the generator. Namely, N random latent codes are sampled to create N activation output vectors at the i^{th} layer. We then conduct UMAP on these N activation vectors to provide a low-rank basis matrix V , and the data mean μ_U . The UMAP coordinates b_j of each activation are then computed by projection: $b_j = V^T(o_j - \mu_U)$. Then we transfer these directions to the latent space z by linear regression. Given an individual basis vector v_k (i.e., a column of V), and the corresponding co-

ordinates $b_{1:N}^i$, where b_j^i is the scalar i^{th} coordinate of b_j . The latent basis vector u_k to identify a latent direction corresponding to this principal component is given as follows: $u_i = \arg \min \sum_j \|u_i k_j^i - z_j\|^2$. Equivalently, the whole basis is computed simultaneously with:

$$U = \arg \min \sum_j \|Uk_j - z_j\|^2 \quad (11)$$

Each column of U then aligns with the variation along the corresponding column of V . The individual dimensions b_i each correspond to different edits in an interpretable manner. Given a new image with latent codes z , manipulation can be conducted by varying the coordinates of x :

$$z' = z + Ub, x' = g(z') \quad (12)$$

Besides StyleGAN and BigGAN, experiments show that ALM yielded useful directions for earlier models, including DCGAN and Progressive GAN, using the BigGAN procedure above.

3.4.2 Attribute Manipulating

Given the directions found with UMAP, we now show that these can be decomposed into interpretable edits

For StyleGAN, layer-wise control of StyleGAN is conducted on the latent codes w^i . We use the notation $D(u_i, j-k)$ to denote edit directions; for example, $D(u_1, 0-3)$ means moving along component u_1 at the first four layers only. $D(u_2, all)$ means moving along component u_2 globally: in the latent space and all layer inputs. A simple user interface can be provided for the exploration of the principal directions in an interactive manner. After computing the directions, the user is free to inspect the effect of any of them by simple slider controls. The layer-wise application is enabled by specifying a start and end layer for which the edits are to be applied. The first ten or so principal components, such as head rotation ($D(u_1, 0-2)$) and lightness/background ($D(u_8, 5)$), operate well in the range $[-2, \dots, 2]$, beyond which the image becomes unrealistic. In contrast, face roundness ($D(u_{37}, 0-4)$) can work well in the range $[-20, \dots, 20]$, when using 0.7 as the truncation parameter. For truncation, we use interpolation to the mean as in StyleGAN. The variation in slider ranges described above suggests that truncation by restricting w to lie within two standard deviations of the mean would be a very conservative limitation on the interface’s expressivity since it can produce interesting images outside this range.

For other GANs that do not support layer-wise edits, e.g., BigGAN, they can be modified to produce behavior similar to StyleGAN. This is conducted by varying the intermediate Skip-z inputs z_i separately from the latent z . Namely, z_i is enabled to vary individually between layers in a direct analogy to the style mixing of StyleGAN. Edits may be performed to the inputs to different layers independently.

3.4.3 Adaptive Perturbation Tuning for Construction of Nature Transformation

To prevent the edited latent codes from going far from the manifold, *Adaptive Perturbation Tuning* (APT) is used to bound the manipulation of the latent codes.

Perturbation noise can be obtained by randomly sampling from $N(0, 1)$ for N_r times and projecting perturbed latent code $\tilde{z}_\phi^{(K)}$ back onto a l_∞ -bounded neighborhood around $\tilde{z}_n^{(0)} : \{z_n \mid \|\tilde{z}_n^{(0)} - z_n\| < \epsilon\}$ where ϵ is set to 0.03.

As a fixed constant, the perturbation threshold ϵ ignores the fact that every data example may have different intrinsic robustness [7]. To address the accuracy-robustness trade-off, adaptive threshold tuning is used to discover a non-uniform and effective perturbation level and the corresponding customized target label for each example. Intuitively, for training samples that are intrinsically closer to the decision boundary, a smaller ϵ will be applied to reduce the generalization error introduced by adversarial training.

The perturbation level ϵ_i allocated to each example x_i is given as

$$\epsilon_i = \underset{\epsilon}{\operatorname{argmin}} \left\{ \max_{\tilde{z}_i \in B(\epsilon, z_i)} f_\theta \neq y_i \right\} \quad (13)$$

Alternative updates are used to update each ϵ_i , i.e., implementing one SGD update on θ , and then updating the ϵ_i in the current batch. Specifically, at each iteration, we conduct the nature transformation with perturbation sensitivity $\epsilon_i + \rho$ where ρ is a constant. If the misclassification occurs, then we keep the current ϵ_i . If not, we increase $\epsilon_i + \rho$ until misclassification occurs or ϵ_i reaches the truncated value to make sure ϵ_i will not be too large. As the transformations are also used to update the model parameter θ , no additional cost is introduced by the adaptive threshold tuning.

Besides, the adaptive label smoothing strategy is also used to reflect different perturbation tolerance on each example. Label smoothing is proposed in [34] to convert one-hot label vectors into one-warm vectors $y = (1 - \alpha)y + \alpha u$ representing low-confidence classification to prevent the model from making over-confident predictions. α is set as $c \times \epsilon_i$ so that a more significant perturbation sensitivity would hold a higher label uncertainty, and c is a hyperparameter. u is set as *Dirichlet*(1), namely Dirichlet distribution on an all one vector [7].

Consequently, the objective function in Equation 1 is updated as

$$\min_{\theta} \frac{1}{n} \sum_{i=1}^n \max_{\substack{T_s, s \in S \\ z_i^s \in B(\epsilon_i, z_i^s)}} L(f_\theta(T_s(x)), \tilde{y}) \quad (14)$$

4. Experiments

4.1. Data and Setup

The performance of NaTra is evaluated on three datasets: LSUN car (resized to 512×512) and cat (256×256) [40], and CelebA-HQ [21, 22] (Face).

We make no modifications to the dataset and use a pre-trained StyleGAN model. For all techniques, we train models using 20 epochs. We evaluate all methods on their ability to classify the smiling attribute, as well as three other attributes. In this experiment, the disentangled latents defining the finer style correspond to resolutions ranging from 128×128 to 1024×1024 . CelebA-HQ contains 30,000 high quality images at 1024×1024 resolution.

We use both standard VGG-16 [32] and WideResNet for robustness performance evaluation. For VGG-16, we implement the standard hyperparameters. For WideResNet, we use the same model structure provided by [26]. We use four existing data augmentation approaches as baselines compared with NaTra: (1) Random perturbation (Random). For an input x , we generate a random variation via adding random noise from $N(0, 1)$ to the latent codes; (2) Adversarial Training (Adv) which minimizes the adversarial risk over l_∞ -norm bounded perturbations of size ϵ_{pixel} in input space; (3) Mixup in the latent space (MixL). It augments data by reconstructing mixed latent codes between the two pairs of inputs; and (4) Mixup in the input space (MixI). It augments data by mixing two pairs of inputs in the input space; (5) NaTra without Latent Codes Expansion (NaTra-OL); (6) NaTra without Adaptive Perturbation Tuning (NaTra-OA); (7) AdvMix [14].

4.2. Robustness Evaluation and Analysis

In this section, we evaluate the robustness of NaTra on benchmark datasets. Finally, we benchmark the state-of-the-art robustness and integrate the unlabeled data for further improvement.

Table 1. Test accuracy on attributes (i.e. with glass, gender, smiling, age and identification, denoted by S1-S4 and ID) classification tasks on Face dataset with different robust enhancements.

Method	Accuracy on Attributes (%)				
	S1	S2	S3	S4	ID
Original	96.82	90.32	84.16	79.76	75.87
Adv	95.86	91.41	84.28	79.81	75.69
MixI	95.92	90.35	84.18	79.96	76.12
MixL	96.91	90.41	84.28	79.81	75.69
Random	97.12	91.56	86.12	81.79	76.16
NaTra-OL	97.56	92.29	85.65	79.47	76.21
NaTra-OA	97.83	92.35	85.72	79.55	76.41
NaTra	98.11	93.10	86.33	80.18	77.02

The robustness evaluations of all data augmentation approaches are shown in Table 1 with respect to the same clas-

Table 2. Test accuracy on classification tasks on LSUN Car and Cat datasets with different robust enhancements.

Method	Accuracy (%)	
	Cat	Car
Original	92.36	90.10
Adv	92.50	91.05
MixI	92.37	89.80
MixL	92.33	89.83
Random	93.25	90.69
NaTra-OL	93.03	91.76
NaTra-OA	93.62	92.14
NaTra	94.15	92.86

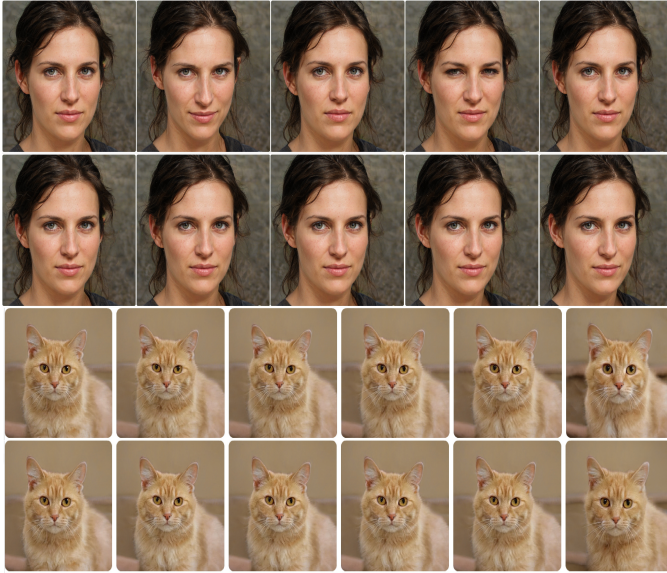


Figure 4. The demonstration of escaped samples that are misclassified by the actual model, and correctly classified by fine-tuning the model via NaTra on natural transformation, i.e., face orientation, eye-opening, facial expression for human, and head elevation and body orientation for cat.

sification task, where “Original” denotes the accuracy on natural test images. Our proposed NaTra achieves the best robustness on both CelebA and LSUN. Particularly, NaTra improves $\sim 8\%$ over Adv, and $\sim 4\%$ even over Mixup. A similar trend of improvement is also observed among NaTra and NaTra-OL and NaTra-OA, which reveals the efficiency of the LCE and Adaptive Perturbation Tuning.

Compared with images of low fidelity, the robustness improvements of NaTra over other baselines are more significant on images of high fidelity. This is because adversarial training on high fidelity is a more challenging problem that may have more misclassified examples during training.

We also evaluate the robustness evaluations of all data augmentation approaches with respect to various classification task in Table 2. It is also confirmed that NaTra systematically achieves high accuracy, namely NaTra can lead to a

lower generalization error.

We find there are a large number of escaped examples of images that are all correctly classified by the actual model, but its transformations are misclassified. After fine-tuning using NaTra, these escaped examples can be correctly classified, as demonstrated in Figure 4.

It is often challenging, if not completely impossible, to collect a large-scale dataset for a certain person, an object, which is essential to train good deep models, e.g., classifiers. To address data limitation, few-shot learning in image generation [42] or fine-tuning to transfer the knowledge of pre-trained models [37] can be applied to train good generator and then implement NaTra. It is also interesting to find that it is feasible to train a face recognition model with more than 95% accuracy when giving only 100 face images for each person.

5. Conclusion

In this paper, we propose NaTra, an adversarial training scheme that is designed to improve the robustness of deep models against customized input variations arising in real world natural transformations. Our framework can be realized by harnessing pre-trained generative models to conduct nature transformations for data augmentation, resulting in controllable attribute edit as well as good reconstruction quality. Experimental results demonstrated that NaTra could relieve the insensitivity to task-irrelevant variations while increasing the deep models’ generalization. We hope this work could advance the implementation of robust deep models in the real world.

References

- [1] Rameen Abdal, Yipeng Qin, and Peter Wonka. Image2stylegan: How to embed images into the stylegan latent space? In *Proceedings of the IEEE international conference on computer vision*, pages 4432–4441, 2019.
- [2] Shumeet Baluja and Ian Fischer. Adversarial transformation networks: Learning to generate adversarial examples. *arXiv preprint arXiv:1703.09387*, 2017.
- [3] David Bau, Jun-Yan Zhu, Hendrik Strobelt, Bolei Zhou, Joshua B Tenenbaum, William T Freeman, and Antonio Torralba. Gan dissection: Visualizing and understanding generative adversarial networks. *arXiv preprint arXiv:1811.10597*, 2018.
- [4] David Bau, Jun-Yan Zhu, Jonas Wulff, William Peebles, Hendrik Strobelt, Bolei Zhou, and Antonio Torralba. Inverting layers of a large generator. In *ICLR Workshop*, volume 2, page 4, 2019.
- [5] Andrew Brock, Jeff Donahue, and Karen Simonyan. Large scale GAN training for high fidelity natural image synthesis. In *International Conference on Learning Representations*, 2019.

- [6] Nicholas Carlini and David Wagner. Towards evaluating the robustness of neural networks. In *2017 IEEE Symposium on Security and Privacy (SP)*, pages 39–57. IEEE, 2017.
- [7] Minhao Cheng, Qi Lei, Pin-Yu Chen, Inderjit Dhillon, and Cho-Jui Hsieh. Cat: Customized adversarial training for improved robustness. *arXiv preprint arXiv:2002.06789*, 2020.
- [8] Antonia Creswell and Anil Anthony Bharath. Inverting the generator of a generative adversarial network. *IEEE transactions on neural networks and learning systems*, 30(7):1967–1974, 2018.
- [9] Ekin D Cubuk, Barret Zoph, Dandelion Mane, Vijay Vasudevan, and Quoc V Le. Autoaugment: Learning augmentation policies from data. *arXiv preprint arXiv:1805.09501*, 2018.
- [10] Logan Engstrom, Dimitris Tsipras, Ludwig Schmidt, and Aleksander Madry. A rotation and a translation suffice: Fooling cnns with simple transformations. *arXiv preprint arXiv:1712.02779*, 1(2):3, 2017.
- [11] Robert Geirhos, Carlos RM Temme, Jonas Rauber, Heiko H Schütt, Matthias Bethge, and Felix A Wichmann. Generalisation in humans and deep neural networks. In *Advances in neural information processing systems*, pages 7538–7550, 2018.
- [12] Ian J Goodfellow, Jonathon Shlens, and Christian Szegedy. Explaining and harnessing adversarial examples. *arXiv preprint arXiv:1412.6572*, 2014.
- [13] Sven Gowal, Chongli Qin, Po-Sen Huang, Taylan Cemgil, Krishnamurthy Dvijotham, Timothy Mann, and Pushmeet Kohli. Achieving robustness in the wild via adversarial mixing with disentangled representations. In *Proceedings of the IEEE/CVF Conference on Computer Vision and Pattern Recognition*, pages 1211–1220, 2020.
- [14] Sven Gowal, Chongli Qin, Po-Sen Huang, Taylan Cemgil, Krishnamurthy Dvijotham, Timothy Mann, and Pushmeet Kohli. Achieving robustness in the wild via adversarial mixing with disentangled representations. In *Proceedings of the IEEE/CVF Conference on Computer Vision and Pattern Recognition*, pages 1211–1220, 2020.
- [15] Jinjin Gu, Yujun Shen, and Bolei Zhou. Image processing using multi-code gan prior. In *Proceedings of the IEEE/CVF Conference on Computer Vision and Pattern Recognition*, pages 3012–3021, 2020.
- [16] Erik Härkönen, Aaron Hertzmann, Jaakko Lehtinen, and Sylvain Paris. Ganspace: Discovering interpretable gan controls. *arXiv preprint arXiv:2004.02546*, 2020.
- [17] Xun Huang and Serge Belongie. Arbitrary style transfer in real-time with adaptive instance normalization. In *Proceedings of the IEEE International Conference on Computer Vision*, pages 1501–1510, 2017.
- [18] Ajil Jalal, Andrew Ilyas, Constantinos Daskalakis, and Alexandros G Dimakis. The robust manifold defense: Adversarial training using generative models. *arXiv preprint arXiv:1712.09196*, 2017.
- [19] Can Kanbak, Seyed-Mohsen Moosavi-Dezfooli, and Pascal Frossard. Geometric robustness of deep networks: analysis and improvement. In *Proceedings of the IEEE Conference on Computer Vision and Pattern Recognition*, pages 4441–4449, 2018.
- [20] Harini Kannan, Alexey Kurakin, and Ian Goodfellow. Adversarial logit pairing. *arXiv preprint arXiv:1803.06373*, 2018.
- [21] Tero Karras, Samuli Laine, and Timo Aila. A style-based generator architecture for generative adversarial networks. In *Proceedings of the IEEE conference on computer vision and pattern recognition*, pages 4401–4410, 2019.
- [22] Tero Karras, Samuli Laine, Miika Aittala, Janne Hellsten, Jaakko Lehtinen, and Timo Aila. Analyzing and improving the image quality of stylegan. In *Proceedings of the IEEE/CVF Conference on Computer Vision and Pattern Recognition*, pages 8110–8119, 2020.
- [23] Alexey Kurakin, Ian Goodfellow, and Samy Bengio. Adversarial machine learning at scale. *arXiv preprint arXiv:1611.01236*, 2016.
- [24] Zachary C Lipton and Subarna Tripathi. Precise recovery of latent vectors from generative adversarial networks. *arXiv preprint arXiv:1702.04782*, 2017.
- [25] Junyu Luo, Yong Xu, Chenwei Tang, and Jiancheng Lv. Learning inverse mapping by autoencoder based generative adversarial nets. In *International Conference on Neural Information Processing*, pages 207–216. Springer, 2017.
- [26] Aleksander Madry, Aleksandar Makelov, Ludwig Schmidt, Dimitris Tsipras, and Adrian Vladu. Towards deep learning models resistant to adversarial attacks. *arXiv preprint arXiv:1706.06083*, 2017.
- [27] Seyed-Mohsen Moosavi-Dezfooli, Alhussein Fawzi, Jonathan Uesato, and Pascal Frossard. Robustness via curvature regularization, and vice versa. In *Proceedings of the IEEE Conference on Computer Vision and Pattern Recognition*, pages 9078–9086, 2019.
- [28] Augustus Odena, Christopher Olah, and Jonathon Shlens. Conditional image synthesis with auxiliary classifier gans. In *International conference on machine learning*, pages 2642–2651, 2017.
- [29] Nicolas Papernot, Patrick McDaniel, Xi Wu, Somesh Jha, and Ananthram Swami. Distillation as a defense to adversarial perturbations against deep neural networks. In *2016 IEEE Symposium on Security and Privacy (SP)*, pages 582–597. IEEE, 2016.
- [30] Guim Perarnau, Joost Van De Weijer, Bogdan Raducanu, and Jose M Álvarez. Invertible conditional gans for image editing. *arXiv preprint arXiv:1611.06355*, 2016.
- [31] Haonan Qiu, Chaowei Xiao, Lei Yang, Xinchun Yan, Honglak Lee, and Bo Li. Semanticadv: Generating adversarial examples via attribute-conditional image editing. *arXiv preprint arXiv:1906.07927*, 2019.
- [32] Karen Simonyan and Andrew Zisserman. Very deep convolutional networks for large-scale image recognition. *arXiv preprint arXiv:1409.1556*, 2014.
- [33] Yang Song, Rui Shu, Nate Kushman, and Stefano Ermon. Constructing unrestricted adversarial examples with generative models. In *Advances in Neural Information Processing Systems*, pages 8312–8323, 2018.
- [34] Christian Szegedy, Vincent Vanhoucke, Sergey Ioffe, Jon Shlens, and Zbigniew Wojna. Rethinking the inception architecture for computer vision. In *Proceedings of the IEEE conference on computer vision and pattern recognition*, pages 2818–2826, 2016.

- [35] Christian Szegedy, Wojciech Zaremba, Ilya Sutskever, Joan Bruna, Dumitru Erhan, Ian Goodfellow, and Rob Fergus. Intriguing properties of neural networks. *arXiv preprint arXiv:1312.6199*, 2013.
- [36] Igor Vasiljevic, Ayan Chakrabarti, and Gregory Shakhnarovich. Examining the impact of blur on recognition by convolutional networks. *arXiv preprint arXiv:1611.05760*, 2016.
- [37] Yaxing Wang, Chenshen Wu, Luis Herranz, Joost van de Weijer, Abel Gonzalez-Garcia, and Bogdan Raducanu. Transferring gans: generating images from limited data. In *Proceedings of the European Conference on Computer Vision (ECCV)*, pages 218–234, 2018.
- [38] Chaowei Xiao, Bo Li, Jun-Yan Zhu, Warren He, Mingyan Liu, and Dawn Song. Generating adversarial examples with adversarial networks. *arXiv preprint arXiv:1801.02610*, 2018.
- [39] Cihang Xie, Yuxin Wu, Laurens van der Maaten, Alan L Yuille, and Kaiming He. Feature denoising for improving adversarial robustness. In *Proceedings of the IEEE Conference on Computer Vision and Pattern Recognition*, pages 501–509, 2019.
- [40] Fisher Yu, Ari Seff, Yinda Zhang, Shuran Song, Thomas Funkhouser, and Jianxiong Xiao. Lsun: Construction of a large-scale image dataset using deep learning with humans in the loop. *arXiv preprint arXiv:1506.03365*, 2015.
- [41] Hongyi Zhang, Moustapha Cisse, Yann N Dauphin, and David Lopez-Paz. mixup: Beyond empirical risk minimization. *arXiv preprint arXiv:1710.09412*, 2017.
- [42] Shengyu Zhao, Zhijian Liu, Ji Lin, Jun-Yan Zhu, and Song Han. Differentiable augmentation for data-efficient gan training. *arXiv preprint arXiv:2006.10738*, 2020.
- [43] Jun-Yan Zhu, Philipp Krähenbühl, Eli Shechtman, and Alexei A Efros. Generative visual manipulation on the natural image manifold. In *European conference on computer vision*, pages 597–613. Springer, 2016.